Morphological transitions and bistability in Turing systems

Teemu Leppänen,[1] Mikko Karttunen,[1] R. A. Barrio,[1,2] and Kimmo Kaski[1]
[1]*Laboratory of Computational Engineering, Helsinki University of Technology, P.O. Box 9203, FIN-02015 HUT, Finland*
[2]*Instituto de Fisica, Universidad Nacional Autónoma de México (UNAM), Apartado Postal 20-364, 01000 México, Distrito Federal, Mexico*

(Received 5 February 2003; revised manuscript received 21 June 2004; published 3 December 2004)

It is well known that in two dimensions Turing systems produce spots, stripes and labyrinthine patterns, and in three dimensions lamellar and spherical structures, or their combinations, are observed. In this paper we study transitions between these states in both two and three dimensions. First, we derive the regions of stability for different patterns using nonlinear bifurcation analysis. Then, we apply large scale computer simulations to analyze the pattern selection in a bistable system by studying the effect of parameter selection on morphological clustering and the appearance of topological defects. The method elaborated in this paper presents a probabilistic approach for studying pattern selection in a bistable reaction-diffusion system.

DOI: 10.1103/PhysRevE.70.066202 PACS number(s): 05.45.−a, 82.40.Ck, 47.54.+r

I. INTRODUCTION

Nature presents a fascinating diversity of patterns in plants, animals and other natural formations as results of complex physico-chemical processes [1]. Alan Turing showed in 1952 that a simple system of coupled reaction-diffusion equations for two chemicals could give rise to finite wavelength spatial patterns due to a mechanism called diffusion-driven instability [2]. These so-called Turing patterns and other related chemical systems have ever since been under intensive theoretical study [3,4] and similar pattern forming mechanisms have been connected to various physical systems such as gas-discharge systems [5,6], irradiated materials [7], catalytic surface reactions [8] and semiconductor nanostructures [9].

Turing systems have also been proposed to account for pattern formation in many biological systems, e.g., color patterns on fish skin [10,11], butterfly wings [12] and lady beetles [13] to mention a few. The first experimental evidence of a Turing structure was not reported until 1990 by Castets *et al.* [14], who observed a sustained standing nonequilibrium chemical pattern in a single-phase open reactor with a chloride-iodide-malonic acid (CIMA) reaction. There has been an increasing interest to develop simple and plausible mathematical models that could describe, at least qualitatively, these pattern formations [15–17].

The forms and variations of patterns generated by Turing systems have been studied analytically and numerically by investigating the conditions for instability [18], assuming inhomogeneous diffusion coefficients [19], by introducing domain curvature [20] or growth [21], and both homogeneous [22] and periodic suppression [23]. In addition, symmetries in Turing systems are of great interest, since they may have biological relevance; see, e.g., Refs. [19,24,25]. On the other hand, chemical experiments have confirmed both theoretical and numerical results and brought more insight concerning the chemical dynamics of dissipative structures [26–28]. Recently, we have studied numerically the effect of dimensionality by simulating three-dimensional Turing systems [29]. The experimental study of three-dimensional Turing structures [30] is rather cumbersome since it is hard to determine the exact three-dimensional structure based on two-dimensional projections. While in two dimensions one obtains spots, stripes or labyrinthine patterns, in three dimensions complex shapes of, e.g., lamellae, spherical droplets and their combinations appear.

Previously, studies of Turing systems have typically concentrated on reaction kinetics and stability aspects (see, e.g. [31–33]), while the issue of pattern structure and its connectivity has received less attention. Here, we focus on connectivity of Turing patterns and its dependence on the parameters of the system. We present a simple way to quantitatively characterize Turing structures and their connectivity based on statistical analysis of the patterns obtained from simulations. The connectivity of a pattern with given parameters cannot be predicted analytically in the presence of bistability of both striped and spotty patterns. We also study the "connectivity transition," which occurs as the parameters of the system are between those giving rise to either monostable spots or stripes.

State selection is a fundamental problem in nonequilibrium physics and appears in very different contexts ranging from driven superconductivity [34] to chemical systems [3,35]. In this paper we address this problem in the context of reaction-diffusion systems [36] and characterize the pattern selection in the presence of a bistability by analyzing the statistical properties of the resulting patterns in systems with different sizes. The transition between monostable patterns can occur only through a bistable regime, where the pattern selection will be shown to be probabilistic. This nonequilibrium transition bears some resemblance to a first order equilibrium phase transition: the system exhibits hysteresis. This phenomenon has been addressed previously in the context of reaction-diffusion systems. Hysteresis has been observed in experimental [37] as well as numerical [38] studies of Turing system, but the transition mechanisms have not been studied in great detail.

This paper is organized as follows. In the next section, we briefly introduce a reaction-diffusion model of the Turing kind (the BVAM model) and in Sec. III we present the relevant results of the nonlinear bifurcation analysis. Then, in Sec. IV we discuss the concept of connectivity in these sys-

tems and the methods for characterizing the transition between different patterns. In Sec. V, we present results from comprehensive numerical simulations. Finally, in Sec. VI we draw some relevant conclusions.

II. THE MODEL

A Turing system models the evolution of the concentrations of two chemicals, or morphogens. It is represented in general by the following reaction-diffusion equations

$$U_t = D_U \nabla^2 U + f(U,V),$$

$$V_t = D_V \nabla^2 V + g(U,V), \tag{1}$$

where $U \equiv U(\vec{x},t)$ and $V \equiv V(\vec{x},t)$ are the morphogen concentrations, and D_U and D_V the corresponding diffusion coefficients setting the time scales for diffusion. The reaction kinetics is described by the two nonlinear functions f and g.

In this study we focus on a Turing model introduced by Barrio *et al.* [11], in which the reaction kinetics is developed by Taylor expanding the nonlinear functions around a stationary solution (U_c, V_c). The Barrio-Varea-Aragon-Maini (BVAM) model is phenomenological one and it is not based on any particular experimental chemical reaction. If terms of the fourth and higher order are neglected, and the remaining equations are nondimensionalized [39], the model reads as

$$u_t = D\nabla^2 u + \nu(u + av - uv^2 - Cuv),$$

$$v_t = \nabla^2 v + \nu(bv + hu + uv^2 + Cuv), \tag{2}$$

where $u = U - U_c$ and $v = V - V_c$ are the concentration fields. Here the parameter C determines the relative strength of the quadratic and cubic nonlinear terms, D is the ratio of the diffusion coefficients of the two chemicals, and ν acts as a scaling factor. Setting $D \neq 1$ is a necessary but not sufficient condition for the diffusion-driven instability to occur in two and three dimensions [40]. For details about the instability and the linear stability analysis of the model we refer the reader to Barrio *et al.* [11,29].

The BVAM model of Eq. (2) has been devised in such a way that one can adjust the relative strength of the quadratic and cubic nonlinearities. These terms dominate the instability by imposing symmetry requirements to the system and thus they dictate the pattern selection. In this way our model is different from the Brusselator [3] or the Lengyel-Epstein [32] models which have only one nonlinear term and the morphology of the resulting pattern is determined by the value of the bifurcation parameter, i.e., the distance to the onset of instability.

From the linear stability analysis [11,29] we obtain the dispersion relation and the conditions for the diffusion-driven instability as the region in k-space with positive growth rate, i.e., eigenmodes $u = u_0 e^{\lambda t}$ and $v = v_0 e^{\lambda t}$ with eigenvalues $\mathrm{Re}\{\lambda(k)\} > 0$. In addition, one can analytically derive the modulus of the critical wave vector

$$k_c^2 = \frac{\nu(Db+1)}{2D}, \tag{3}$$

which has here been determined for the case $h = -1$ (set to obtain only one stable state at $u = v = 0$ in the absence of diffusion). By parameter adjustment it is possible to allow only a few unstable modes, which can be done with several different parameter sets. Based on the linear analysis we chose two sets of parameters for the numerical calculations. First, $D = 0.516$, $a = 1.112$, $b = -1.01$ and $\nu = 0.45$ for the critical wave number $k_c = 0.46$, and second, $D = 0.122$, $a = 2.513$, $b = -1.005$ and $\nu = 0.199$ corresponding to $k_c = 0.86$. In a discretized three-dimensional cubic system there is more mode degeneracy than in two dimensions, since the wave number is of the form

$$|\vec{k}| = \frac{2\pi}{L}\sqrt{n_x^2 + n_y^2 + n_z^2}, \tag{4}$$

where L is the system size and n_x, n_y, n_z are the wave number integer indices (in a two-dimensional system $n_z = 0$).

III. NONLINEAR ANALYSIS

The linear stability analysis that we discussed briefly above is able to render only a partial picture of the phase space behavior of inherently nonlinear Turing systems. In fact one can expect a wide variety of stable patterns with different symmetries formed in the system. In order to get a better insight to the nonlinear effects of the system we extend the analysis from the linear to the weakly nonlinear regime. The latter is often called bifurcation analysis and it yields analytical forms for the amplitudes of different symmetries [41,42]. The aim of the bifurcation analysis is to find a description of the concentration field $\vec{w} = (u,v)$ in terms of the active Fourier modes, i.e.,

$$\vec{w} = \vec{w}_0 \sum_{\vec{k}_j} (W_j e^{i\vec{k}_j \cdot \vec{r}} + W_j^* e^{-i\vec{k}_j \cdot \vec{r}}), \tag{5}$$

where $\vec{w}_0$ defines the direction of the active modes and W_j and W_j^* are the amplitudes for modes $\vec{k}_j$ and $-\vec{k}_j$, respectively. Notice that the sum of complex conjugates is real. The unstable modes have slow dynamics, whereas the stable modes relax quickly and are said to be slaved to the unstable modes.

We have carried out full nonlinear analysis of the BVAM model by mapping the dynamics of the chemical system to an equivariant amplitude space using the center manifold reduction method [43]. The amplitude equation system consists of equations for all the unstable modes which are of the following form

$$\frac{dW_j}{dt} = \lambda_c W_j + f_j(W_1, \ldots, W_n), \tag{6}$$

where the exact form of the term $f_j(W_1, \ldots, W_n)$ depends on the lattice under study. The eigenvalue λ_c may be written in the vicinity of the onset of instability by using a linear approximation

$$\lambda_c = \left.\frac{d\lambda}{da}\right|_{a=a_c}(a-a_c) = \frac{\nu^2(\nu-2R)}{[\nu(1+b)-2R][\nu-R]}, \quad (7)$$

where $R=Dk_c^2=\nu(Db+1)/2$.

The application of bifurcation analysis to two-dimensional reaction-diffusion systems has become almost a routine procedure [4,44]. However, the three-dimensional case is much more challenging. Pattern selection in a three-dimensional chemical system is not straightforward, but there are multiple possible states that must be taken into account depending on the symmetry under study. The lattices typically studied in three dimensions are simple cubic (sc), body-centered cubic (bcc) and face-centered cubic (fcc). Callahan and Knobloch have been among the first to study three-dimensional pattern selection using nonlinear analysis under all these different symmetries [45–47]. In this study we have followed their computational procedure to calculate the coefficients of the amplitude equations [47]. The fact that the strength of the nonlinearities (C) governs the pattern selection in the BVAM model necessitates some additional algebraic manipulations since we have to find the stability as a function of the nonlinear coefficient C.

In a two-dimensional Turing system the patterns of interest are typically either stripes aligned in parallel or spots organized in a hexagonal lattice. Depending on the system parameters, one of these patterns may spontaneously arise from random initial conditions in computer simulations. The bifurcations are thus studied in a hexagonal lattice defined by three unit wave vectors k_i separated by an angle of $2\pi/3$. Since the base vectors of the hexagonal lattice are not linearly independent ($-k_1-k_2=k_3$) the lattice is said to exhibit resonant modes, i.e., the coupling of two other modes may have effects on the growth of the third mode. Then, the amplitude equation system corresponding to the two-dimensional hexagonal lattice of the critical mode k_c is defined the normal form given by

$$\frac{dW_j}{dt} = \lambda_c W_j + \Gamma W_{j+1}^* W_{j+2}^* - g[|W_j|^2 + \kappa(|W_{j+1}|^2 + |W_{j+2}|^2)]W_j, \quad (8)$$

where $j=1, 2, 3$ (mod 3) and the coefficients Γ, g and κ can be presented in terms of the parameters of the original reaction-diffusion system [Eq. (2)]. This is done by carrying out a rigorous calculation using the center manifold reduction, which yields

$$\Gamma = \frac{-2bC\nu R\sqrt{\nu(\nu-2R)}}{(\nu+b\nu-2R)\sqrt{(\nu+b\nu-2R)(\nu-R)}}, \quad (9)$$

$$g = \frac{3b\nu^2(\nu-2R)R}{(\nu+b\nu-2R)^2(\nu-R)}, \quad (10)$$

$$\kappa = 2, \quad (11)$$

where we have denoted $R=Dk_c^2=\nu(Db+1)/2$. The linear coefficient of Eq. (8) is given by Eq. (7).

After derivation of the parameters [Eqs. (9)–(11)] one must analyze the stability of the bifurcating branches. In two dimensions there is one branch corresponding to stripes with stationary amplitudes $W_1^c=\sqrt{(\lambda_c/g)}e^{i\phi_1}$ and $W_2^c=W_3^c=0$. When $k_c=0.86$ the stability analysis predicts this branch to be stable for $C<0.161$. On the other hand, there are two equilateral branches of hexagons defined by

$$|W_1^c| = |W_2^c| = |W_3^c| = \frac{-\Gamma \pm \sqrt{\Gamma^2 + 4\lambda_c g[1+2\kappa]}}{2g(1+2\kappa)}, \quad (12)$$

where the parameters are those defined by Eqs. (9)–(11). The branch corresponding to the plus sign in Eq. (12) is always unstable. The other branch of hexagons is predicted to be stable for $0.084<C<0.611$. Since the center manifold reduction evaluates the dynamics by weakly nonlinear approximation, the results of the analysis may be questioned for strong nonlinearities corresponding to large values of C. Based on extensive numerical simulations we have found that the hexagonal phase is undoubtedly stable even for $C=1.57$. However, the most important result of the bifurcation analysis is the region of bistability is predicted to be $0.084<C<0.161$. Within this parameter domain both stripes and hexagonal spotty patterns are predicted to be stable for $k_c=0.86$.

In a three-dimensional Turing system the structures that have been studied numerically are planar lamellae, hexagonally packed cylinders (HPC) and spherical shapes organized in a bcc symmetry, which have been obtained in simulations of the Brusselator model [48,49]. These structures are stable also in the BVAM model of Eq. (2) if they are the initial configuration of the system, but recently we have shown that the system cannot always find these perfect states, when the simulation is started from random initial conditions [29]. We are particularly interested in the structures formed by self-organization from an arbitrary initial state due to their suggested relevance to morphogenesis. From a random initial state in three dimensions we were not able to obtain spherical shapes organized in a perfect lattice. Furthermore, planar lamellar structures have not been obtained from random initial state, but instead found complex minimal surfaces [29].

Next we approximate the three-dimensional pattern selection by considering an sc lattice, which is a coarse approximation for the forming symmetry. We have also carried out bifurcation analysis for the bcc lattice, but it does not seem to serve as a good approximation for the structures resulting from random initial conditions [39]. In the sc lattice there are no resonant modes and the amplitude equations are defined by

$$\frac{dW_j}{dt} = \lambda_c W_j - g[|W_j|^2 + \kappa(|W_{j+1}|^2 + |W_{j+2}|^2)]W_j, \quad (13)$$

where again $j=1, 2, 3,$ (mod 3) and g and κ are the coefficients given by

$$g = \frac{-b\nu^2[C^2(8\nu-23R)-27R](\nu-2R)}{9(\nu+b\nu-2R)^2(\nu-R)}, \quad (14)$$

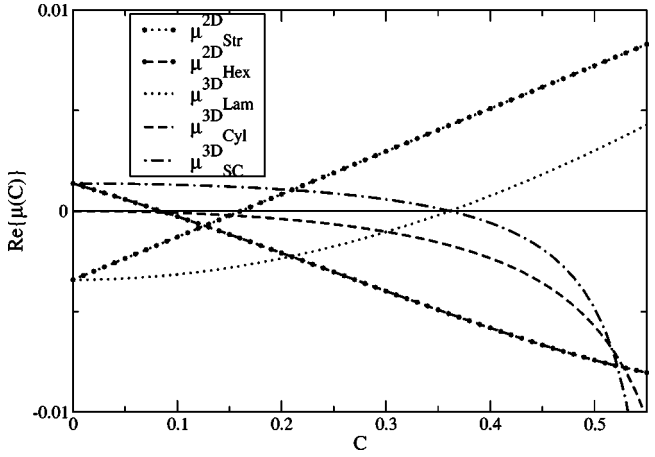

FIG. 1. The set of eigenvalues $\mu(C)$ determining the stability of different structures, i.e., the stripes and hexagonal patterns in 2D, and lamellae, cylinders, and sc droplets in 3D. The symmetries are stable for $\mu(C)<0$.

$$\kappa = \frac{18[C^2(8\nu - 7R) - 3R]}{C^2(8\nu - 23R) - 27R}, \tag{15}$$

where R is the same as before, and the linear coefficient of Eq. (13) is given by Eq. (7).

The branch corresponding to planar lamellae is given by the stationary amplitudes $|W_1^c| = \sqrt{\lambda_c/g}$, $W_2^c = W_3^c = 0$ and predicted to be stable for $C < 0.361$. For the square packed cylinders, which in an sc lattice correspond to the HPC structures [49], one obtains the amplitudes $|W_1^c| = |W_2^c| = \sqrt{\lambda_c/g(\kappa+1)}$, $W_3^c = 0$ and the stability for all $C < 0.650$. The isotropic branch of spherical structures in an sc lattice has the amplitudes $|W_1^c| = |W_2^c| = |W_3^c| = \sqrt{\lambda_c/g(2\kappa+1)}$ and is predicted to be stable for $0.361 < C < 0.589$. It should be noted that the analysis does not predict bistability of lamellar and spherical structures. On the other hand, the cylindrical phase is predicted to be stable for all C.

In Fig. 1 we have collected the eigenvalues of the linearized amplitude systems in 2D and 3D obtained from Eqs. (8) and (13), respectively. The most relevant outcome of bifurcation analysis is that it predicts the stability of different symmetries and the parameter domain, where the system exhibits bistability. The exact morphology selection within the bistable domain cannot be predicted, which is why we employ a new connectivity measure to be introduced in the next section. An additional inadequacy of the bifurcation analysis is that in three dimensions it cannot predict the stability of more general three-dimensional structures such as twisted grain boundaries [49] or periodic minimal surfaces [29], which arise in simulations started from random initial conditions.

For a more detailed discussion of topics related to nonlinear analysis, we refer the reader to a more technical paper by one of us [39]. In this study, we perform numerical calculations in which we vary the parameter C [in Eq. (2)] that controls the appearance of either stripes or spots. By gradually changing this control parameters we observe a transition from stripes (2D) or lamellar (3D) structures to spots (2D) or spherical droplet (3D) structures as predicted by the bifurcation analysis. The transition and the pattern selection within the bistable transition regime will be characterized by concentrating on the connectivity of the structures defined below.

IV. CONNECTIVITY

Numerical calculations were performed using a standard Euler method (see the next paragraph for details). In the numerical simulations of Eq. (2) one deals with two concentration fields with characteristic wave lengths. In order to visualize this, the concentration of only one of the chemicals is typically plotted with a gray scale, since in these systems the fields are in antiphase, i.e., if there is a large amount of chemical U in some subdomain, the concentration of chemical V would be low there. These concentration fields vary continuously having diffuse boundaries. Now, the connectivity of chemicals in the system can be studied by defining subdomains dominated by either chemical U or V, provided that the amplitude of the pattern is large enough. If we define the boundary as the interface between subdomains dominated by different chemicals, we can easily locate the boundaries, where the concentrations change rapidly, typically within one or two lattice sites of the discretized system. Now, if two points belong to the same domain, i.e., are not separated by a boundary, they are considered connected. The definition of the boundaries in this way is only conceptual in the sense that in the U-dominated domains the concentration of V does not have to be zero, only much less than the concentration of U.

In this study the numerical simulations were carried out by discretizing the spatial dimensions into a square (2D) or cubic cell (3D) lattice and calculating the Laplacians [53] in Eq. (2). In these types of problems the finite difference scheme and Euler's method are often employed [11,26,54]. It is possible, and sometimes even desirable, to use the Euler's method since it is fast and stable under appropriate conditions, which can be checked by simple linear stability analysis. The Euler scheme has been shown to be stable for our model even in such circumstances as a disk, where step control was needed [25]. In all our simulations we chose the spatial discretization to be $dx = dy = dz = 1.0$ and the equations of motion were integrated in time using the time step $dt = 0.05$. The resolution of the spatial discretization did not affect the pattern selection provided that the characteristic wave length of the pattern was set to be a multiple times the lattice constant (dx). The boundary conditions were chosen to be periodic and the initial concentrations of the chemicals were Gaussian perturbations around the trivial stationary state (0,0) with a variance significantly lower than the amplitude of the final patterns. In order to study the connectivity in two- and three-dimensional Turing patterns, we performed extensive simulations for system sizes up to 5×10^5 lattice cells and let the system to evolve up to 2×10^6 time steps in order to reach a stationary state.

In Fig. 2 we show changes in the two-dimensional concentration fields for different values of the quadratic nonlinear coefficient C in Eq. (2). The patterns in Fig. 2 are snap-

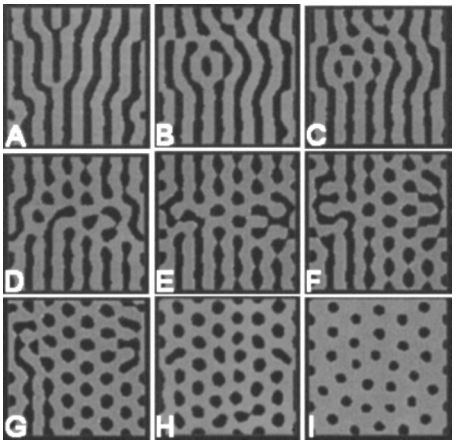

FIG. 2. Transition from stripes to spots. The patterns obtained after 50 0000 iterations in a 100×100 system with $k_c=0.45$. Black corresponds to areas dominated by chemical U (zeros) and the lighter color chemical V (ones). C varies from 0.007 to 1.000 from A to I.

shots taken after 50000 iterations in order to make the transition more gradual and visible within a wider parameter range. This causes the patterns not being perfectly symmetric and leads to distortions. If one continued simulations for an indefinitely long time, Figs. 2(A)–2(E) would most likely evolve towards aligned stripes, whereas Figs. 2(F)–2(I) would evolve towards a hexagonal lattice of spots, i.e., the presented patterns are transient.

When the cubic term dominates (small C), the resulting stationary pattern is striped with a small number of imperfections, see Fig. 2(A). These imperfections can be considered as topological defects, or dislocations, which could serve as nucleation sites for spots. More dislocations appear [see Figs. 2(B) and 2(C)] when the relative strength of the quadratic term is made larger. As the quadratic term grows, more spots nucleate and they arrange themselves to hexagonal structure and at the same time getting rid of the remaining stripes [see Figs. 2(F)–2(H)]. Similar nucleation processes have earlier been observed in numerical simulations of a reaction-diffusion system generating dissipative quasiparticles [50]. Finally, when the quadratic term is enhanced even further, and only spots remain [Fig. 2(I)]. As the present discussion concerning the nucleation of structure is purely qualitative it should be mentioned that, e.g., Hagberg and Meron have previously employed a more rigorous approach [51]. They studied the dynamics of curved fronts in bistable two-dimensional media using a set of kinematic equations.

In this sequence of simulations the transition from stripes to spots was enforced by using a single control parameter C. Nevertheless, the transition from striped to spotty pattern seems to happen quite abruptly with respect to C. Note that the difference in parameters between the figures is not constant: From A to I, $C=0.007$, 0.091, 0.116, 0.124, 0.129, 0.135, 0.169, 0.258, 1.000. In this context and for $k_c=0.45$ the bistability is predicted to occur for $0.073<C<0.139$, as discussed in [39] in more detail. This corresponds to Figs. 2(B)–2(F).

Now, let us discuss the patterns in Fig. 2 from the clustering point of view. In order to simplify this without loss of generality, we can assign zeros and ones to the whole lattice based on the chemical that dominates a given domain. With this mapping we consider the number of clusters, which is calculated using the well-known Hoshen-Kopelman algorithm [52] as in typical percolation problems. In Fig. 2(A) one can see that in the case of stripes the number of U- and V-dominated clusters is almost the same, and both types are extended dominantly in one of the dimensions (both chemicals have percolated). However, in the case of a spotty structure [Fig. 2(I)], chemical U appears as separate round clusters or spots, whereas chemical V forms one connected cluster (V has percolated). Between these two limiting cases there is the transition region, depicted in Figs. 2(D)–2(F), where U-dominated clusters appear as spots and stripes in the form of a "string-of-pearls."

In order to compare the numbers of clusters N_c^d for systems of different size, we normalize it by dividing with N_c^d, where $N_c=k_cL/2\pi$, L denotes the linear system size (square or cube in 2D or 3D), and d the spatial dimension. N_c^d is the maximum number of spherically symmetric clusters in a d-dimensional system as if the clusters were uniformly distributed and the effect of boundaries was neglected. Due to the periodicity of the chemical structure, the number of clusters in the d-dimensional system can be estimated to be $N^d=(N_c+1/2)^d$. However, an additional correction is required to take into account the effect of boundaries. Now, one can estimate the number of additional partial clusters due to boundaries by approximating the length (area) of the boundary and the number of clusters within this domain (dN^{d-1}). As a result of this discussion we propose the scaling function for the number of clusters to be

$$F_d[N(C),N_c]=\frac{N(C)}{N_c^d}\left(1-\frac{d}{N_c+\frac{1}{2}}\right), \tag{16}$$

where $N(C)$ is the calculated number of clusters for control parameter C. By revising the Hoshen-Kopelman algorithm one could have directly calculated the number of clusters by taking periodicity into account, in which case Eq. (16) reduces to $F_d(N(C),N_c)=N(C)/N_c^d$. However, this approach was not implemented and the normalization was carried out by using the Eq. (16).

In the following section we will present the results of our numerical simulations. We have studied the connectivity or the number of clusters in the patterns as a function of the control parameter C, which adjusts the morphology selection between stripes and spots.

V. SIMULATION RESULTS

The first result is shown in Fig. 3, where we have plotted the number of U clusters, calculated using the Hoshen-Kopelman algorithm, as a function of the nonlinear parameter C in Eq. (2). Here we did not start from random initial configuration, but used instead the final configuration of the previous simulation as the initial configuration for the next simulation and let the pattern stabilize for 250 000 iterations. In this way we could change the control parameter C continuously and observe hysteresis (the direction is shown by

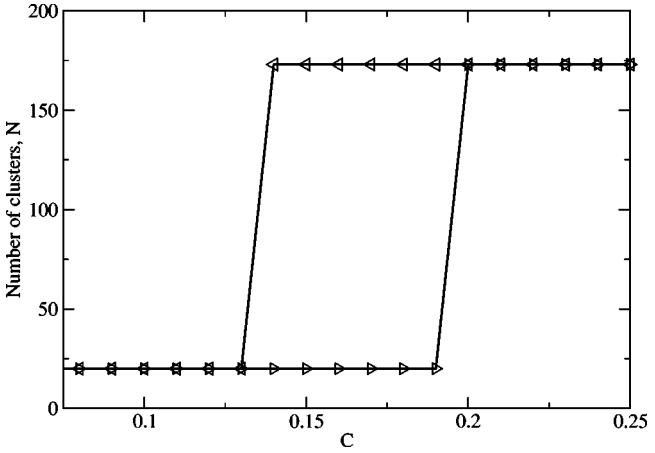

FIG. 3. The number of U clusters as a function of the nonlinear parameter C, which was varied continuously throughout the sweep in a single simulation. The two-dimensional 100×100 pattern was given 250 000 iterations for stabilization at each value of C ($k_c=0.86$). The arrow heads describe the direction of the sweep implying hysteresis.

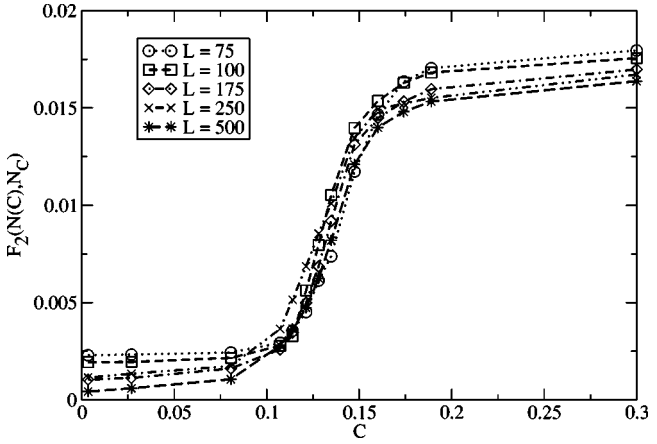

FIG. 4. The normalized number of U clusters as a function of C in two-dimensional systems. System sizes are $L=75$, $L=100$, $L=175$, $L=250$, and $L=500$. The results were averaged up to 20 simulations and they match with the analytical prediction for the bistable regime given by $0.084<C<0.161$.

the arrows in Fig. 3) characterized by the number of clusters. It should be noted that as the control parameter is changed continuously, the present symmetry tends to persist. The bifurcation analysis discussed before predicted that the bistability for $0.084<C<0.161$, with which our numerical result shown in Fig. 3 does not match precisely. For longer simulation times the hysteresis loop tended to become even wider, i.e., the bistability region widens.

The hysteresis has recently been observed while studying the space-averaged density of one substance in a one-dimensional reaction-diffusion system as a function of a feeding parameter [55]. We observe similar behavior also with respect to the amplitude of the concentration wave in the Turing system as earlier [37,56]. We suggest that a transition exhibiting hysteresis can be further characterized by measuring the number of clusters in the case of reaction-diffusion systems forming spatial patterns. In addition to the hysteresis effect we have also observed a slowing down of the dynamics while the parameter C approaches the parameter region corresponding to morphological changes. For bistable C values the system requires more simulation steps to achieve the final steady state. This has been studied earlier both numerically [57] and experimentally [37,58] in bistable chemical systems.

The competition between hexagonal spotty patterns and stripe patterns has previously been addressed in the field of pattern formation both experimentally [37,59] and numerically [38,60–62]. These studies do not, however, provide a method to investigate the morphological changes, but only corroborate the analytically predicted existence of both symmetries. In the following, we will try to find some insight into the morphological transition resulting in from the bistability of stripes and hexagonal spots. In order to study the transition we employ extensive numerical simulations and measure the number of clusters. The results were averaged over up to 20 simulations for each value of C. We carried out studies for several system sizes in order to guarantee the generalizable nature of our results.

In Fig. 4 we plot the averaged scaling function $F_2(N(C),N_c)$ for U-clusters against C for several different system sizes. The simulations were started from random initial configurations of the chemicals for each value of C. Neglecting the number of V-clusters does not affect our conclusions, since the curves would be symmetrical (number of V clusters goes to 1 for high C). From Fig. 4 one can clearly see that the transition takes place at those values of the parameter C for which bifurcation analysis predicted the system to be bistable (see Sec. III) and indeed the number of clusters characterizes the transition. In addition, it can be seen that the normalization function of Eq. (16) scales the number of clusters in such a way that the results for different system sizes agree within reasonable deviations.

The smoothness of the curve in Fig. 4 as compared to the data plotted in Fig. 3 is due to averaging. The boundaries of the hysteresis loop in Fig. 3 are not well-defined and the transition in a single simulation may take place for any value of C within the region of bistability. Thus Fig. 4 can be thought of as a normalized sum of steplike functions. In a system exhibiting bistability one cannot predict the exact transition value for the control parameter C. Based on Fig. 4, however, it can be proposed that the predictions of the bifurcation analysis have the power to approximate the dynamics of a bistable pattern forming system in a probabilistic manner. For example for $C=0.15$ the bifurcation analysis predicts a bistability, but based on our simulation results, we suggest that when the system is initialized to a random state it will tend to evolve towards a hexagonal spotty pattern.

If one carries out the simulations for very small system sizes, finite-size effects can be observed. For small system sizes the $F_2(N(C),N_c)$ curves become more steep in the transition region and the value C for which the transition takes place seems to be affected by the finite size of the system. This would suggest that in the limit of small systems, the transition would become almost discontinuous. However, the system cannot be made infinitely small since the (periodic) boundary conditions start to affect the behavior of the sys-

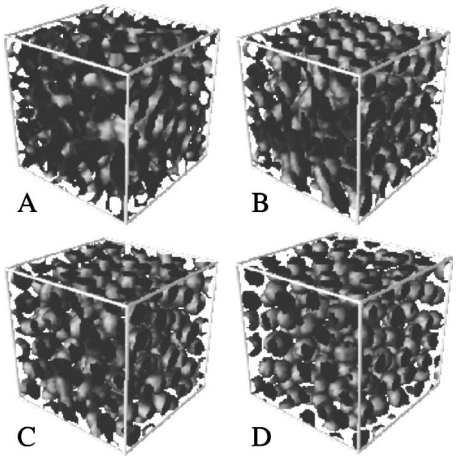

FIG. 5. Transition from a twisted minimal surface to spherical shapes in a three-dimensional system of size $50\times50\times50$. The structures were obtained after 500 000 iterations with $k_c=0.86$. The visualization was carried out by plotting the middle concentration isosurface. Parameter values: (A) $C=0$, (B) $C=0.44$, (C) $C=0.53$, and (D) $C=1.0$

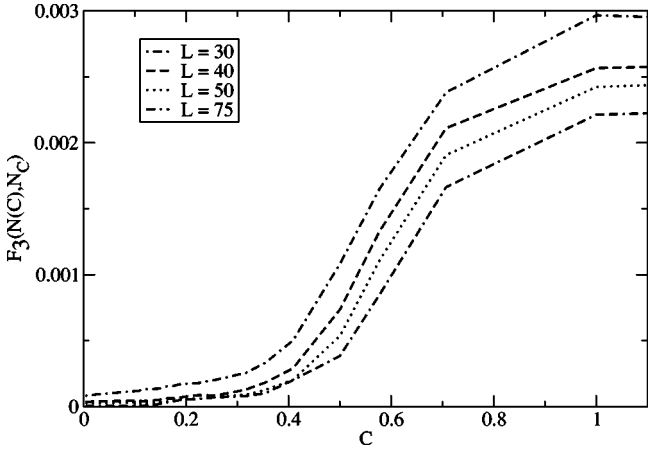

FIG. 6. The averaged normalized number of U clusters as a function of C in a three-dimensional systems. System sizes are $L=30$, $L=40$, $L=50$, and $L=75$. The bifurcation analysis predicts unstable lamellar structures and stable sc droplets for $C>0.361$, whereas stable cylindrical structures are predicted for all $C<0.65$.

tem. As discussed earlier the spots tend to nucleate from topological defects, or dislocations, of the striped pattern, i.e., from the points where the stripes coincide (Fig. 2). In the case of a small system even one dislocation can affect the morphology of the whole system and thus quickly transform stripes into a lattice of spots. In a larger system many dislocations have to appear at various sites to give rise to spots which in turn make the appearance of more spots favorable.

So far we have discussed our simulation results in 2D systems but we have also studied the connectivity transition extensively in 3D. In this case stripes and spots become lamellae and spherical droplets, respectively. Figure 5 shows the concentration isosurfaces obtained in computer simulations with random initial configuration for four different values of C. From Fig. 5 one can observe that in three dimensions one cannot obtain pure planar lamellae or organized spherical structures (FCC, BCC or HPC) spontaneously from random initial conditions. The lamellae we obtain in three dimensions is a periodic continuous, aligned and crossing lamellae without local organization and it resembles a minimal surface solution [see Fig. 5(A)]. The characterization of the various surfaces is difficult, but luckily the specific organization of qualitatively similar structures does not significantly affect the measured clustering in the structures. The fact that the cylindrical phase is predicted to be stable in sc lattice for all parameter values C makes the structure selection even more complicated, especially in the transition region.

It is supposed that in 3D the transition does not occur at the same point with respect to C as in 2D since the third dimension gives to the clustering process one more degree of freedom, and thus it is easier for the structures to connect. This is indeed what one finds. Figure 6 depicts the normalized number of clusters for four different system sizes. One can see that the behavior of the system is different from that in two dimensions. Now, the transition occurs at a higher value of C, since a relatively smaller cubic nonlinear coupling favoring lamellar structures is sufficient for increasing connectivity in three-dimensional space.

The bifurcation analysis does not predict very well the transition domain in the three-dimensional case. The stable lamellae was predicted to change to stable spherical droplets at $C=0.355$, which corresponds to the border of the transition region in Fig. 6. The cylindrical structures were predicted to be stable for all C, which results in a bistability. The insufficient nature of the bifurcation analysis may further be explained by the sc-lattice approximation. On the other hand, the stability of twisted lamellar surfaces could not be analyzed under any symmetry condition. Unlike in 2D we did not observe any finite-size effects for the smallest possible system sizes.

VI. CONCLUSIONS

In this study, we have investigated the connectivity of spatial patterns generated by the reaction-diffusion mechanism both in 2D and 3D. This was done by applying clustering analysis for the dominating chemical. The numerical simulations were consistent with the predictions drawn from the bifurcation analysis, and the system showed a transition in the proximity of the predicted C-value irrespective of the individual system size. The agreement with theory turned out to be closer in the 2D case than in 3D, since in 2D there is a simple transition between monostable patterns through a bistable regime. In 3D the analytical prediction of the changes in connectivity was more difficult, since it predicted the system to be bistable for all parameter values and no bistability was predicted between lamellar and spherical structures in the sc lattice. On the other hand, for the bcc lattice the bifurcation analysis did predict a bistability, but the bistable values of the control parameter did not agree with the results of the numerical simulations as well as the predictions for an sc lattice. Although the bcc structures are stable in Turing systems, it seems that the system cannot find them when the simulation is started from a random initial

configuration. In large systems of dissipative quasiparticles this kind of behavior has been hypothesized to be due to an instability of transient structures [50].

The bistability of two different patterns is observed in a variety of chemical [4] and biological systems [17,63]. The approach of this study brought more insight into the pattern selection in Turing systems. We have shown that at least in the context of Turing systems the pattern selection of a bistable system can be predicted probabilistically. By this we mean that although one cannot determine in advance the trajectory in the phase space based on the parameters, one may give approximate estimates for the state selection as the structure develops from random initial conditions. We have also shown that the nonequilibrium morphological transition has characteristics similar to first order phase transition, i.e., hysteresis is observed. The hysteresis can be seen not only with respect to the amplitude of the chemical concentration as earlier, but also with respect to the morphological changes, i.e., the averaged number of clusters.

The fact that the system size does not affect the clustering and the pattern selection at all (given that system is not too small) implies that the Turing mechanism is very general and it is applicable to systems of various sizes. Also the facts that the pattern selection can be predicted probabilistically as the evolution starts from random initial conditions and that the established patterns tend to persist even under conditions for which they are not predicted to be stable could be important for morphogenesis.

ACKNOWLEDGMENTS

We wish to thank János Kertész for helpful discussions. One of us (R.A.B.) wishes to thank the Laboratory of Computational Engineering at Helsinki University of Technology for its hospitality. This work has been supported by the Academy of Finland through its Centre of Excellence Program (T.L. and K.K.) and Grant No. 00119 (M.K.). Financial support from project IN101702 from CONACyT (R.A.B.), the Finnish Academy of Science and Letters (T.L.) and Jenny and Antti Wihuri foundation (T.L.) are also gratefully acknowledged.

[1] P. Ball, *The Self-Made Tapestry: Pattern Formation in Nature* (Oxford University Press, Oxford, 2001).
[2] A. M. Turing, Philos. Trans. R. Soc. London, Ser. B **237**, 37 (1952).
[3] G. Nicolis and I. Prigogine, *Self-Organisation in Non-Equilibrium Chemical Systems* (Wiley, New York, 1977).
[4] R. Kapral and K. Showalter, *Chemical Waves and Patterns* (Kluwer Academic, Dordrecht, 1995).
[5] H. G. Purwins, C. Radehaus, and J. Berkemeier, Z. Naturforsch., A: Phys. Sci. **43a**, 17 (1988).
[6] E. Ammelt, Yu. A. Astrov, and H. G. Purwins, Phys. Rev. E **58**, 7109 (1998).
[7] D. Walgraef and N. M. Ghoniem, Phys. Rev. B **67**, 064103 (2003).
[8] J. Falta, R. Imbihl, and M. Henzler, Phys. Rev. Lett. **64**, 1409 (1990).
[9] J. Temmyo, R. Notzel, and T. Tamamura, Appl. Phys. Lett. **71**, 1086 (1997).
[10] S. Kondo and R. Asai, Nature (London) **376**, 678 (1995).
[11] R. Barrio, C. Varea, J. L. Aragón, and P. Maini, Bull. Math. Biol. **61**, 483 (1999).
[12] T. Sekimura, A. Madzvamuse, A. J. Wathen, and P. Maini, Proc. R. Soc. London, Ser. B **267**, 851 (2000).
[13] S. S. Liaw, C. C. Yang, R. T. Liu, and J. T. Hong, Phys. Rev. E **64**, 041909 (2002).
[14] V. Castets, E. Dulos, J. Boissonade, and P. De Kepper, Phys. Rev. Lett. **64**, 2953 (1990).
[15] H. Haken, *Synergetics, An Introduction* (Springer-Verlag, Berlin, 1977).
[16] H. Meinhardt, *Models of Biological Pattern Formation* (Academic, New York, 1982).
[17] J. D. Murray, *Mathematical Biology* (Springer-Verlag, Berlin, 1993).
[18] L. Szili and J. Toth, Phys. Rev. E **48**, 183 (1993).
[19] R. A. Barrio, J. L. Aragón, M. Torres, and P. K. Maini, Physica D **168–169**, 61 (2002).
[20] C. Varea, J. L. Aragón, and R. A. Barrio, Phys. Rev. E **60**, 4588 (1999).
[21] C. Varea, J. L. Aragón, and R. A. Barrio, Phys. Rev. E **56**, 1250 (1997).
[22] T. Leppänen, M. Karttunen, K. Kaski, and R. A. Barrio, Prog. Theor. Phys. Suppl. **150**, 367 (2003).
[23] M. Dolnik, A. M. Zhabotinsky, and I. R. Epstein, Phys. Rev. E **63**, 026101 (2001).
[24] B. Hasslacher, R. Kapral, and A. Lawniczak, Chaos **3**, 7 (1993).
[25] J. L. Aragon, M. Torres, D. Gil, R. A. Barrio, and P. K. Maini, Phys. Rev. E **65**, 051913 (2002).
[26] M. Dolnik, I. Berenstein, A. M. Zhabotinsky, and I. R. Epstein, Phys. Rev. Lett. **87**, 238301 (2001).
[27] P. Borckmans, G. Dewel, A. De Wit, E. Dulos, J. Boissonade, F. Gauffre, and P. De Kepper, Int. J. Bifurcation Chaos Appl. Sci. Eng. **12**, 2307 (2002).
[28] P. De Kepper, E. Dulos, J. Boissonade, A. De Wit, G. Dewel, and P. Borckmans, J. Stat. Phys. **101**, 495 (2000).
[29] T. Leppänen, M. Karttunen, K. Kaski, R. A. Barrio, and L. Zhang, Physica D **168–169**, 35 (2002).
[30] J. J. Perraud, K. Agladze, E. Dulos, and P. De Kepper, Physica A **188**, 1 (1992).
[31] S. L. Judd and M. Silber, Physica D **136**, 45 (2000).
[32] I. Lengyel and I. R. Epstein, Proc. Natl. Acad. Sci. U.S.A. **89**, 3977 (1992).
[33] B. Rudovics, R. Barillot, P. W. Davies, E. Dulos, J. Boissonade, and P. De Kepper, J. Phys. Chem. A **103**, 1790 (1999).
[34] M. Karttunen, K.R. Elder, M.B. Tarlie, and M. Grant, Phys. Rev. E **66**, 026115 (2002).
[35] R. Landauer, Phys. Rev. A **12**, 636 (1975).
[36] S. Metens, G. Dewel, P. Borckmans, and R. Engelhardt, Euro-

phys. Lett. **37**, 109 (1997).
[37] Q. Ouyang, Z. Noszticzius, and H.L. Swinney, J. Phys. Chem. **96**, 6773 (1992).
[38] V. Dufiet and J. Boissonade, Physica A **188**, 158 (1992).
[39] T. Leppänen (unpublished); www.lce.hut.fi/research/polymer/turing_review.pdf
[40] J.A. Vastano, J.E. Pearson, W. Horsthemke, and H.L. Swinney, Phys. Lett. A **124**, 320 (1987).
[41] A. C. Newell, T. Passot, and J. Lega, Annu. Rev. Fluid Mech. **25**, 399 (1993).
[42] M. Ipsen, L. Kramer, and P. G. Sorensen, Phys. Rep. **337**, 193 (2000).
[43] J. D. Crawford, Rev. Mod. Phys. **63**, 991 (1991).
[44] D. Walgraef, *Spatio-temporal Pattern Formation* (Springer-Verlag, New York, 1997).
[45] T. K. Callahan and E. Knobloch, Phys. Rev. E **53**, 3559 (1996).
[46] T. K. Callahan and E. Knobloch, Nonlinearity **10**, 1179 (1997).
[47] T. K. Callahan and E. Knobloch, Physica D **132**, 339 (1999).
[48] A. De Wit, G. Dewel, P. Borckmans, and D. Walgraef, Physica D **61**, 289 (1992).
[49] A. de Wit, P. Borckmans, and G. Dewel, Proc. Natl. Acad. Sci. U.S.A. **94**, 12765 (1997).
[50] A. W. Liehr, M. Bode, and H.-G. Purwins, in *High Performance Computing in Science and Engineering*, edited by S. Wagner (Springer, New York, 2001), p. 425.
[51] A. Hagberg and E. Meron, Phys. Rev. Lett. **78**, 1166 (1997).
[52] J. Hoshen and R. Kopelman, Phys. Rev. B **14**, 3438 (1976).
[53] M. Patra and M. Karttunen, report: www.lce.hut.fi/research/polymer/downloads/stencil_paper.pdf
[54] M. Karttunen, N. Provatas, T. Ala-Nissila, and M. Grant, J. Stat. Phys. **90**, 1401 (1998).
[55] A. Rakos, M. Paessens, and G.M. Schutz, Phys. Rev. Lett. **91**, 238302 (2003).
[56] V. Dufiet and J. Boissonade, J. Chem. Phys. **96**, 664 (1991).
[57] J.M. Reyes de Rueda, G.G. Izús, and C.H. Borzi, J. Stat. Phys. **97**, 803 (1999).
[58] N. Ganapathisubramanian and K. Showalter, J. Phys. Chem. **87**, 1098 (1983).
[59] Q. Ouyang and H.L. Swinney, Nature (London) **352**, 610 (1991).
[60] J. Verdasca, A. De Wit, G. Dewel, and P. Borckmans, Phys. Lett. A **168**, 194 (1992).
[61] P. Borckmans, A. De Wit, and G. Dewel, Physica A **188**, 137 (1992).
[62] O. Jensen, V. O Pannbacker, G. Dewel, and P. Borckmans, Phys. Lett. A **179**, 91 (1993).
[63] B. N. Nagorcka and J. R. Mooney, IMA J. Math. Appl. Med. Biol. **9**, 249 (1992).